Indian Journal of Chemical Technology
Vol. 31, January 2024, pp. 95-104
DOI: 10.56042/ijct.v31i1.7605

# Nickel(II) removal from wastewater by magnetic nanoparticles loaded carbon prepared from *Morinda citrifolia* seed

Ramasamy Sudha[1]*, Rajendran Jayalakshmi[1], KumarappanLatha[2] & Panneerselvam Anitha[3]

[1]Departent of Chemistry, Vivekanandha College of Arts and Sciences for Women (Autonomous), Elayampalayam, Tiruchengode-637 205, Tamil Nadu, India

[2]Department of Chemistry, Vivekanandha College of Technology for Women, Elayampalayam,Tiruchengode-637 205, Tamil Nadu, India

[3]Centre for Research, Department of Chemistry, Government College of Engineering, Salem-636 011, Tamil Nadu, India

*E-mail: drsudha@vicas.org

*Received 16 October 2022; accepted 24 November 2023*

The Ni(II) removal capacity of magnetic nanoparticle loaded carbon derived from *Morinda citrifolia* (MMCSC) seed as compared to pure *Morinda citrifolia* seed powder (MCS) has been evaluated by varying different parameters such as contact time, pH and adsorbent dose during batch adsorption processes. Surface morphology, elemental analysis and functionality of the synthesized materials are characterized by SEM, EDX and FT-IR. The equilibrium data were found to fit well in the Langmuir isotherm. The monolayer adsorption capacity of CMC and MNCMC onto Ni(II) ions are found to be 45.50 and 266.67 mg $g^{-1}$, respectively . The thermodynamic parameters indicated that the adsorption process is spontaneous and exothermic in nature. A single-stage batch adsorber is designed to estimate the amount of adsorbent required to treat the known volume of the effluent using the Langmuir adsorption isotherm. Regeneration study showed that MNCMC could be effectively utilized for the removal of Ni(II) ions for seven cycles of operation under study when compared with CMC.

**Keywords:** Adsorption isotherm, Magnetic nanoadsorbent, *Morinda citrifolia* seed, Nickel(II) removal

## Introduction

In recent years, rapid development of industrial activities have exceeded the discharge of industrial effluent containing heavy metals are released into surface and underground water, which has resulted in a number of environmental problems. Nickel is highly toxic and nonbiodegradable. It has been largely used in the modern industry from where get transferred to the soils and then to plants and animals. Human beings are getting exposed to nickel pollution through the food chain[1,2]. The major sources of nickel contamination to water comes from industrial process such as electroplating, battery and accumulator manufacturing, stainless steel, ceramic, mining and metallurgy, porcelain enamelling and forging[3]. The US Environmental Protection Agency and Bureau of Indian Standards emphasized the presence of nickel not to exceed 0.015 mg $L^{-1}$ in drinking water[4-6]. Therefore, it is very important to develop effective technologies to treat heavy metal polluted wastewater before their discharge into natural environment.

A numerous technology have been developed for removal of nickel(II) from aqueous solution such as ion exchange, chemical precipitation, coagulation and floatation, electrochemical treatment and reverse osmosis[7-10]. However, these technologies require expensive treatment and disposal of secondary toxic metal sludge is very difficult when nickel is present even at very low concentrations. At present, scientists have been considered adsorption by magnetic activated carbon is an efficient, effective and economical method for wastewater purification. The synthesis of magnetic nanoparticle loaded activated carbon prepared from various agricultural waste such as orange rind[11], *citrus limon* wood[12], palm shells[13], palm kernel shells[14],orange peel[15], vine shoots[16], coconut shells[17], corncob[18], Bauhinia purpurea pods[19] and pomegranate peel[20] have been successfully used for the removal of heavy metal ions from aqueous solution.

The aim of the present research is to synthesize magnetic *Morinda citrifolia* seed based carbon to develop a new magnetic adsorbent and study its efficiency for the removal of nickel(II) ions from aqueous solution and wastewater. The synthesized magnetic adsorbents are characterized by FT-IR, SEM

and EDX. The maximum nickel(II) removal ability of nanoadsorbent was optimised by various factors of contact time, pH, adsorbent dose and temperature using batch experiment. The adsorption isotherms, kinetics and thermodynamic parameters for the adsorption Ni(II) ions on nanoadsorbent are also determined in order to estimate the adsorption process. A single-stage batch adsorber was designed for different carbon dose/ effluent volume ratios using the Langmuir equation. The suitability of prepared nanoadsorbent was examined by collecting the wastewater sample from nearby industrial area in Perunduari, Erode district.

## Experimental Section

### Reagents and preparation of adsorbent

#### *Preparation of the Ni(II) solutions*

A stock solution of Ni(II) (100 mg $L^{-1}$) was prepared by dissolving 0.4479 g of AR $NiSO_4 \cdot 6H_2O$ in 1000 mL of deionized water. Nickel(II) solutions with the desired concentrations were prepared by diluting the stock solution. The pH of the solution were adjusted using 0.1 N HCl or 0.1 N NaOH solutions. The nickel-plating industry wastewater was collected from M/S Metal platers in Erode, India.

#### *Preparation of Morinda citrifolia seed powder (MCS)*

*Morinda citrifolia* seed was collected from local area in Salem district, Tamil Nadu, India. The collected raw material was washed carefully with deionised water to remove dust particles and other impurities. The collected raw materials was dried in a hot air oven at 100 ℃ for 4 h and crushed into powder and stored in a bottle and referred as *Morinda citrifolia* seed powder (MCS).

#### *Synthesis of magnetic nanoparticle loaded Morinda citrifolia seed based carbon (MMCSC)*

About, 10 g of anhydrous ferric chloride ($FeCl_3$) and 5 g of ferrous chloride ($FeCl_2.6H_2O$) was mixed in 200 mL of distilled water and stirring vigorously at 80℃ for 30 min. Then 12 g of powered *Morinda citrifolia* seed was added and the solution was stirred for 1 h. Then 20 mL of 25% NaOH solution was added in drop wise and stirring was continued until the black coloured precipitate was obtained. The precipitate was filtered and dried at 100℃ for 12 h. The resultant impregnated samples were activated at 450℃ for 3 h in a muffle furnace. After cooling, the activated sample were washed with deionised water until the pH of the filtrate was about 6-7, and dried in hot air oven for 6 h at 110℃. The obtained samples were named as magnetic *Morinda citrifolia* seed based carbon (MMCSC) and stored in a bottle then used for further experiments.

### Batch adsorption experiment

Batch studies were conducted in polythene bottles of 300 mL capacity. 100 mL of the solution containing 10 mg $L^{-1}$ of the Ni(II) ions was taken in bottles. All the solutions were adjusted to the desired pH and equilibrated for specific periods of time in a temperature-controlled mechanical shaker. At definite time intervals, separation of the adsorbent and solution was carried out by filtration and the residual metal ion concentrations were analysed using an atomic absorption spectrophotometer. Triplicate runs of each test were conducted and the obtained data have been found to vary to less than 1% suggesting the accuracy of the results. The nickel(II) removal (%) was calculated using the following equation:

$$\text{Removal (\%)} = \frac{C_0 - C_e}{C_0} \text{X } 100 \quad \ldots(1)$$

where $C_0$ and $C_e$ are the initial and equilibrium concentrations (mg $L^{-1}$) of the metal ions, respectively.

### Adsorption isotherms

Adsorption isotherms were recorded with 10-60 mg $L^{-1}$ of Ni(II) solutions by adding 0.1 g of adsorbent and equilibrated for 24 h at room temperature. The residual concentration of Ni(II) ions in the solution was measured by AAS. The amount of Ni(II) ions adsorbed at equilibrium, $q_e$ (mg $g^{-1}$), was calculated by the following relationship:

$$q_e = \frac{(C_0 - C_e)V}{m} \quad \ldots(2)$$

where, V is the volume (L) of Ni(II) solution and m is the mass (g) of the adsorbent. The adsorption isotherm indicates how the adsorbate molecules distribute between the liquid phase and the solid phase at equilibrium. The analysis of the isotherm data by fitting them into different isotherm models is an important step to find the suitable model that can be used for designing the process. The experimental data were applied to the two and three parameter non-linear isotherm models: namely Freundlich, Langmuir, Temkin, Redlich-Peterson, Sips, and Dubinin-Radushkevich.

#### *Freundlich isotherm*

The Freundlich isotherm is suitable for a highly heterogeneous surface and expressed by the following equation[21]:

$$q_e = K_F C_e^{1/n} \quad \ldots(3)$$

where, $K_F$ is Freundlich constant ((mg $g^{-1}$)(L $mg^{-1}$) $^{(1/n)}$) related to the bonding energy and n (g $L^{-1}$) is a measure of the deviation from linearity of adsorption. This value indicates the degree of non-linearity between solution concentration and adsorption as follows: if n=1, adsorption is linear; if n<1, adsorption is a chemical process; if n>1, adsorption is a physical process.

***Langmuir isotherm***

The Langmuir model is obtained under the ideal assumption of totally homogenous adsorption surface and represented as follows[22]:

$$q_e = \frac{q_m K_L C_e}{1+K_L C_e} \quad \ldots(4)$$

where, $q_m$ ($mgg^{-1}$) is the maximum monolayer adsorption capacity, and $K_L$ (L $mg^1$) Langmuir constant relating to adsorption energy. The essential characteristics of the Langmuir isotherm parameters can be used to predict the affinity between the sorbate and sorbent using separation factor or dimensionless equilibrium parameter, "$R_L$", expressed as in the following equation[23]:

$$R_L = \frac{1}{1+K_L C_0} \quad \ldots(5)$$

where, $K_L$ is the Langmuir constant and $C_0$ is the initial concentration of Ni(II) ions. The value of $R_L$ indicated the type of Langmuir isotherm to be irreversible ($R_L$=0), favourable (0<$R_L$<1), linear ($R_L$=1), or unfavourable (($R_L$>1).

***Temkin isotherm***

The Temkin isotherm model[24] contains a factor that explicitly takes into account adsorbing species-adsorbate interactions. This model assumes that the heat of adsorption of all the molecules in the layer decreases linearly with coverage due to adsorbent-adsorbate interactions, and the adsorption is characterized by a uniform distribution of binding energies, up to a maximum binding energy. The Temkin isotherm has been applied in the following form:

$$q_e = B \ln(AC_e) \quad \ldots(6)$$

where, A ($Lmg^{-1}$) is the equilibrium binding constant that corresponds to the maximum binding energy, and B is a Temkin constant related to the heat of adsorption (kJ $mol^{-1}$).

***Redlich-Peterson isotherm***

The Redlich-Peterson[25] isotherm is an empirical isotherm incorporating three parameters. It combines both Langmuir and Freundlich equations and the mechanism of adsorption is a hybrid and does not follow ideal monolayer adsorption. The equation is given as:

$$q_e = \frac{K_R C_e}{1+a_R C_e^g} \quad \ldots(7)$$

where, $K_R$ (L $g^{-1}$) and $a_R$ (L $mg^{-1}$) are Redlich-Peterson isotherm constants and g is an exponent that lies between 0 and 1. For g=1, the equation converts to the Langmuir isotherm; for g=0, it simplifies to Henry's law equation; and for$1<<a_R C_e^g$ it is identical with the Freundlich isotherm.

***Sips isotherm***

Sips isotherm[26] is a combined form of Langmuir and Freundlich expressions used for predicting the heterogeneous adsorption systems and circumventing the limitation of the rising adsorbate concentration associated with Freundlich isotherm model. It can be written in the following form:

$$q_e = q_{max}\frac{K_s C_e^{\gamma}}{1+K_s C_e^{\gamma}} \quad \ldots(8)$$

where, $q_{max}$ (mg $g^{-1}$) is the Sips maximum adsorption capacity, $K_s$ (L $mg^{-1}$) the Sips equilibrium constant, and $\gamma$ is the Sips model exponent.

***Dubinin-Radushkevich isotherm***

The Dubinin-Radushkevich isotherm is applied to find out the adsorption mechanism based on the potential theory assuming a heterogeneous surface. Dubinin-Radushkevich isotherm is expressed as follows[27]:

$$q_e = q_{mD}\, e^{-\beta\varepsilon^2} \quad \ldots(9)$$

where, $q_{mD}$ (mg $g^{-1}$) is the Dubinin-Radushkevich monolayer capacity, $\beta$ is a constant related to sorption energy, and $\varepsilon$ is the Polanyi potential which is related to the equilibrium concentration as follows

$$\varepsilon = RT\ln\left[1+\frac{1}{C_e}\right] \quad \ldots(10)$$

where, R is the gas constant (8.314 J $mol^{-1}$ K) and T is the absolute temperature. The constant $\beta$ gives the mean free energy, E, of sorption per molecule of the sorbate when it is transferred to the surface of the solid from infinity in the solution and can be computed using the relationship:

$$E = \left[\frac{1}{\sqrt{2\beta}}\right] \quad \ldots(11)$$

The magnitude of E is used to determine the type of adsorption mechanism, When one mole of ions is transferred to the adsorbent surface, its value is less than 8 kJ $mol^{-1}$ which indicates physical adsorption[28], the value of E is between 8 and 16 kJ $mol^{-1}$, indicates the adsorption process follows ion-exchange[29] while its value in the range of 20-40 kJ $mol^{-1}$ indicates chemisorptions[30].

## Results and Discussion

### FT-IR analysis

The FT-IR spectral data for MCS and MMCSC before and after Ni(II) adsorption are shown in Fig. 1a and b, respectively. The spectra for MCS and MMCSC contained broad, intense peaks at 3398 and 3400 $cm^{-1}$, respectively, that correspond to OH stretching. The peaks around at 1745 $cm^{-1}$ are attributed to the C=O stretching vibration of the carboxylic acid group[31]. At the same time as comparing the both raw and magnetic activated carbon, there are various functional group values are shifted on the surface of MMCSC and Fe-O group[32] is observed at a frequency of 559.36 $cm^{-1}$. The FTIR spectra of Ni(II) ions loaded MCS and MMCSC show that the peaks are shifted slightly from their original arrangement and their values of intensity are also distorted. From the above results clear that the hydroxyl and carboxylic acid groups in MCS, in addition to that Fe-O groups are present in MMCSC, which is responsible for the adsorption of Ni(II) ions.

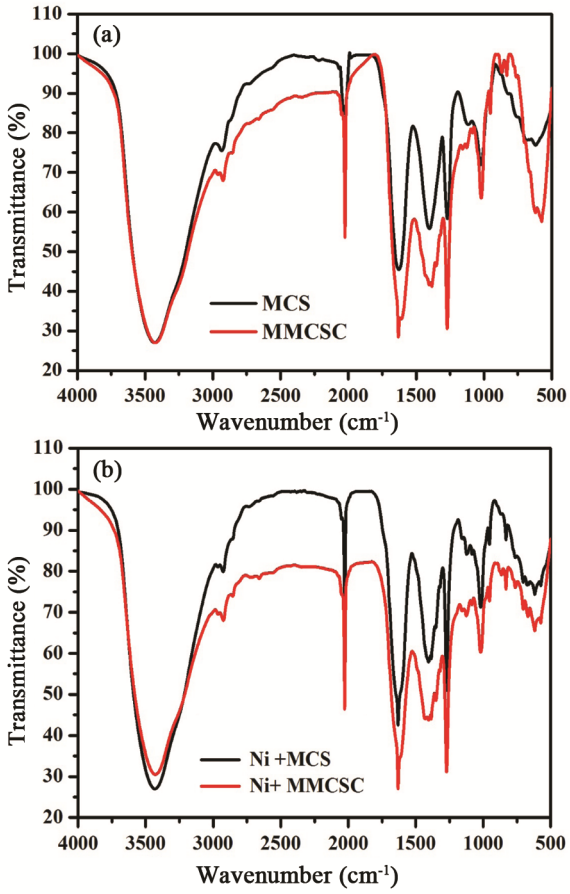


Fig. 1 — FTIR spectra of (a) MCS and MMCSC before adsorption (b) after the adsorption of Ni(II) ions

### SEM- EDX analysis

The SEM image of Fig. 2a and b reveal the porous structure of the MCS and MMCSC surfaces. Comparing the SEM images of the MCS and MMCSC before and after adsorption demonstrates that the metal ions are adsorbed, as confirmed with an EDX analysis. After adsorbing the metal ions, the pores on MCS and MMCSC are covered. The EDX spectra of the Ni(II) ions adsorbed on MCS and MMCSC shows that the peaks for the metal ions in addition to the other cations, confirming the adsorption of Ni(II) ions on the surface of the adsorbent (Fig. 2c and d).

### Effects of contact time

The effect of contact time on the removal of Ni(II) ions from aqueous solutions in the concentration of 10 mg $L^{-1}$ at pH 5.0 and 27°C is shown in Fig. 3. The results obtained from the removal of Ni(II) ions onto the MCS and MMCSC showed that the adsorption increases with increase in contact time. The rate of removal is higher in the beginning due to the large number of available adsorption sites on the adsorbent for the removal of Ni(II) ions. From Fig. 3, it was observed that the time necessary to reach the equilibrium with 2 h for MMCSC and 3 h for MCS. Hence the optimum equilibrium was taken as 2 h for MMCSC and 3 h for MCS in the subsequent experiments.

### Effect of solution pH

Fig. 4 clearly indicates that the adsorption characteristics are highly pH-dependent and maximum removal of 92 ± 0.3% nickel(II) ions onto MMCSC was achieved over a pH range of 4.0-7.0. However, in the case of MCS the maximum nickel(II) removal was found to be 42 ± 0.3 % at pH of 7.0. It has been observed that under at low pH, the amount of metal ion adsorption was very small, because the active adsorption sites remain protonated. As pH

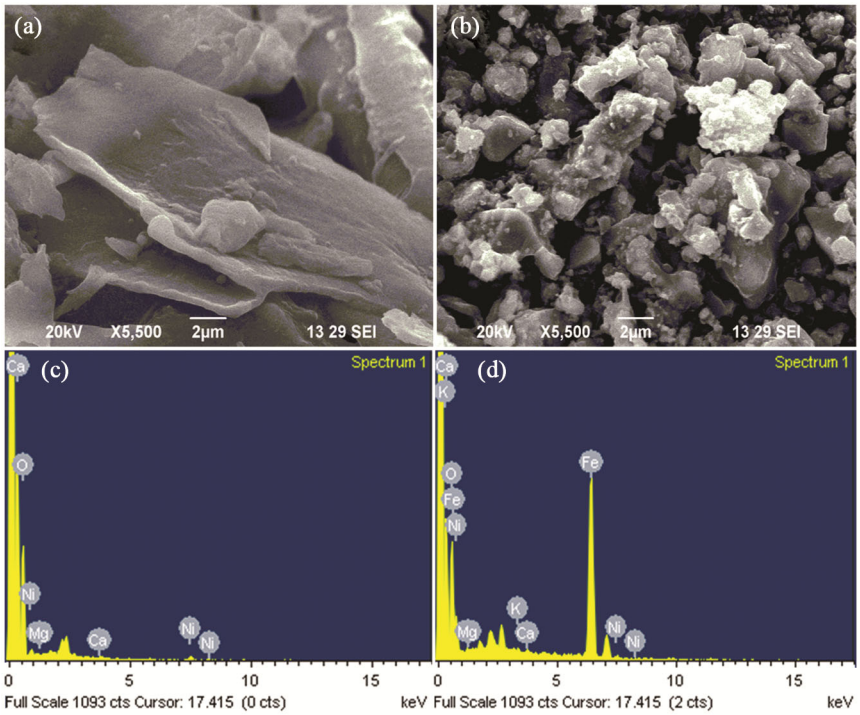


Fig. 2 — (a & b) SEM images and (c & d) EDX patterns of MCS and MMCSC, respectively after Ni(II) adsorption

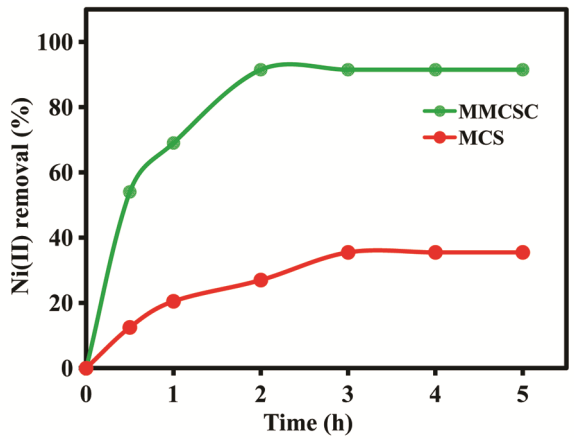


Fig. 3 — Effect of contact time on Ni(II) removal by MCS and MMCSC

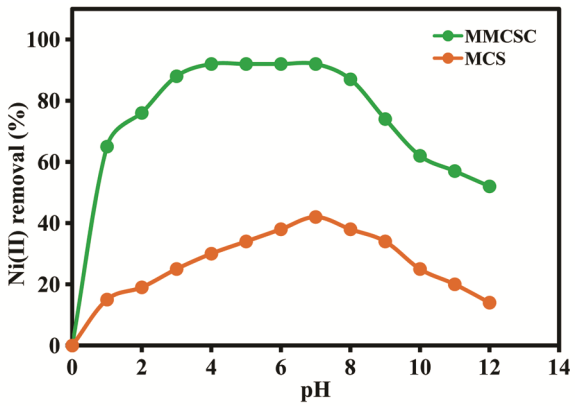


Fig. 4 — Effect of pH on Ni(II) removal by MCS and MMCSC

increases, the concentration of $H^+$ ions decreased, hence they do not complete with metal ions on the adsorption sites, the more adsorption surface with negative charge will easily attract the positively charged metal ions. At higher pH, metal hydroxide starts precipitating from the solution, making actual adsorption studies impossible[33,34]. Therefore, further experiments were carried out at an optimum pH value of 6.0 for MMCSC and in the case of MCS, the optimum pH value was taken as 7.0 for the removal of nickel(II) ions. The influence of solution pH on Ni(II) removal can be explained in terms of zero point charge of the adsorbent. The point of zero charge ($pH_{pzc}$) was determined by the solid addition method[35]. The $pH_{pzc}$ of MMCSC in distilled water is found to be 6 (Figure not given) showing that surface is positively charged below pH 6. Therefore, at high pH value (above 6) Ni(II) species mainly present as $Ni(OH)^+$ and $Ni(OH)_2$ were sorbed (due to micro precipitation).

**Effect of adsorbent dose**

From economic point of view, it is essential to study the influence of adsorbent dose to determine the minimum weight of adsorbent required for the effective removal of metal ions. The effect of adsorbent dose was studied for the adsorption of 100 mL of solution containing the concentration of

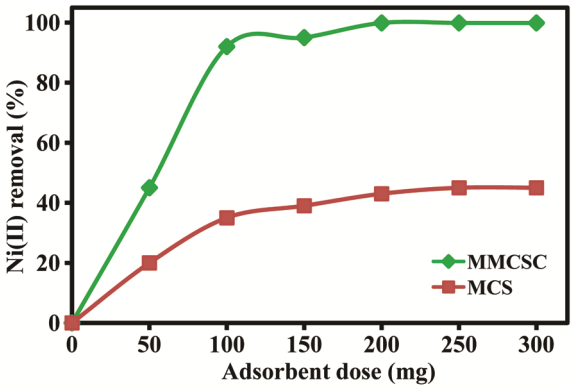


Fig. 5 — Effect of amount of MCS and MMCSC on removal of Ni(II) ions

10 mg $L^{-1}$ of nickel(II) ions, MMCSC and MCS dose range from 50-300 mg at an optimum pH and contact time of 2 h for MMCSC and 3 h for MCS (Fig. 5).

The results shown in Fig. 5, indicates that adsorption increased with increasing adsorbent dose up to a certain value and then became almost constant. It was observed that a minimum MMCSC dose of 100 mg is required for the maximum removal of 99.9 ± 0.1% Ni(II) ions. However, in the case of MCS, the maximum Ni(II) removal of 45 ± 0.2% is obtained by a dose of 250 mg. This may be due to the fact that higher the dosage of adsorbent greater the availability of surface area and the functional groups for metal ions. These chemical groups play an important role in the formation of van der Waals bonding as the functional groups play the main role in binding metals to the adsorbent during adsorption process. This provides more possibilities for adsorption to occur since there was less competition between metals for the binding sites. The above result indicates that MMCSC is 2.5 times more effective than MCS with respect to adsorbent dose.

**Adsorption isotherms**

The isotherm constants, correlation coefficients ($R^2$), sum of squares error (SSE) and root mean squared error (RMSE) values were estimated from the plot of $q_e$ versus $C_e$ (Fig. 6a and b) and are listed in Table 1. The $R^2$ values closer to 1 and small SSE, RMSE values indicate better curve fitting. Based on the $R^2$, SSE and RMSE values from Table 1, the Langmuir, Redlich-Peterson and Sips isotherm model exhibited a better fit for MCS and MMCSC to the adsorption Ni(II) ions, respectively. It can be noted that the Redlich-Peterson and Sips model fit was superimposed on the Langmuir fit (Fig. 6a and b). The Redlich-Peterson and Sips exponent g and γ values in

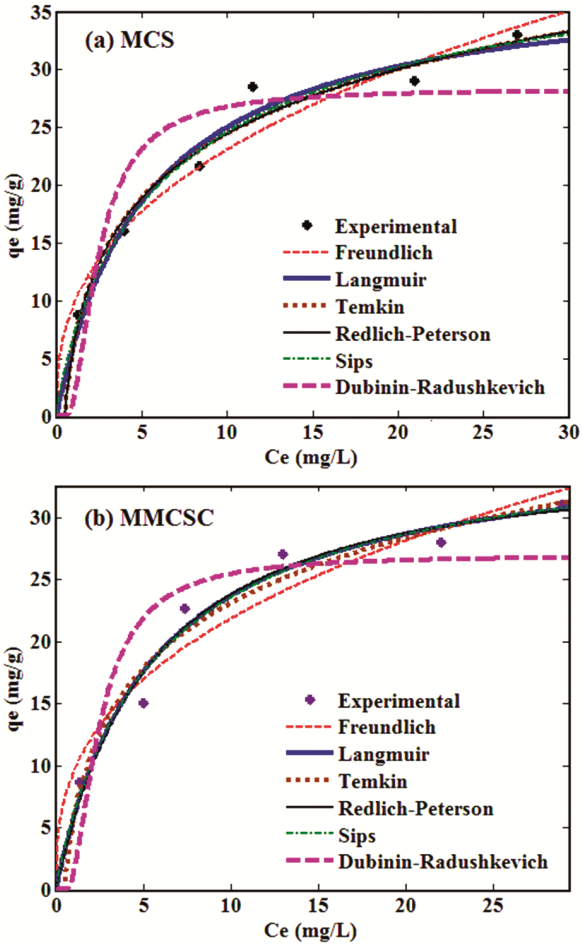


Fig. 6 — Nonlinear isotherms for the adsorption of Ni(II) ions onto (a) MCS and (b) MMCSC

Table 1 are closer to 1 for MCS and MMCSC, which means that the Langmuir isotherm is preferably happening. Hence, the good fit of equilibrium data in Langmuir isotherm expression for MCS and MMCSC confirms the monolayer adsorption of Ni(II) ions. According to Langmuir isotherm, the adsorption capacity ($Q_m$) of Ni(II) ion was found to be 266.67 mg $g^{-1}$ for MMCSC, which was about 5.8 times greater than that of MCS (45.50 mg $g^{-1}$). Furthermore, the $R_L$ values for the Langmuir isotherm fall between 0 and 1 (Table 1), indicating a favourable adsorption of Ni(II) on MCS and MMCSC. The calculated E values of the present study is below 8 kJ $mol^{-1}$, which indicates that the adsorption of Ni(II) ions onto the MCS and MMCSC follows physical adsorption type. Therefore, the adsorption of Ni(II) ions onto MCS and MMCSC surface is a complex, involving more than one mechanism.

The comparison of maximum monolayer adsorption capacity of Ni(II) ions onto various

Table 1 — Nonlinear fitting isotherm parameters for the adsorption of Ni(II) onto MCS and MMCSC

| Isotherm model | Parameter | MCS | MMCSC |
|---|---|---|---|
| Freundlich | $K_F$((mg g$^{-1}$) | 9.633 | 9.463 |
| | n | 2.631 | 2.748 |
| | $R^2$ | 0.943 | 0.922 |
| | SSE | 24.11 | 28.78 |
| | RMSE | 2.455 | 2.682 |
| Langmuir | $q_m$(mg g$^{-1}$) | 45.50 | 266.67 |
| | $K_L$ (L mg$^{-1}$) | 0.188 | 0.184 |
| | $R^2$ | 0.970 | 0.965 |
| | SSE | 13.08 | 13.13 |
| | RMSE | 1.857 | 1.812 |
| | $R_L$ | 0.347-0.081 | 0.352-0.083 |
| Temkin | A | 2.116 | 2.091 |
| | B | 3.482 | 3.299 |
| | $R^2$ | 0.965 | 0.956 |
| | SSE | 14.57 | 16.38 |
| | RMSE | 1.909 | 2.017 |
| Redlich-Peterson | $K_R$(L g$^{-1}$) | 8.793 | 6.398 |
| | $a_R$(L mg$^{-1}$) | 0.319 | 0.156 |
| | g | 0.907 | 0.947 |
| | $R^2$ | 0.969 | 0.964 |
| | SSE | 13.79 | 13.07 |
| | RMSE | 2.088 | 2.087 |
| Sips | $q_{max}$(mg g$^{-1}$) | 42.52 | 37.15 |
| | $K_s$ (L mg$^{-1}$) | 0.146 | 0.178 |
| | γ | 0.849 | 0.925 |
| | $R^2$ | 0.968 | 0.964 |
| | SSE | 13.97 | 13.06 |
| | RMSE | 2.098 | 2.086 |
| Dubinin-Radushkevich | $q_{mD}$(mg g$^{-1}$) | 28.32 | 26.95 |
| | $\beta$(mg$^2$ J$^{-1}$) | 1.854x10$^{-7}$ | 1.936x10$^{-7}$ |
| | E (kJ mol$^{-1}$) | 1.642 | 1.607 |
| | $R^2$ | 0.773 | 0.759 |
| | SSE | 95.52 | 89.28 |
| | RMSE | 4.887 | 5.237 |

adsorbents is presented in Table 2. The value of Ni(II) ions sorption observed in the present study is in good agreement with values found by other researchers. Differences of metal uptake are due to the properties of each adsorbent such as structure, functional groups and surface area. Therefore, it could be concluded that the MMCSC has a promising adsorbent for the removal of Ni(II) from aqueous solutions.

**Effect of temperature and thermodynamic parameters**

The adsorption of Ni(II) ions on MCS and MMCSC was investigated as a function of temperature and the maximum removal of Ni(II) ions was obtained at 27°C. The batch adsorption studies

Table 2 — Monolayer adsorption capacities in the literature for Ni(II) adsorption.

| Adsorbent | $q_m$ (mg g$^{-1}$) |
|---|---|
| Mangosteen shell[36] | 57.14 |
| Citrus Limettioides peel[34] | 38.46 |
| Passion fruit shell[37] | 182.67 |
| Lemon and orange seeds[38] | 118.02 |
| Papaya peel carbon[39] | 32.25 |
| Sugar beet pulp[40] | 9.36 |
| Cucumismelo peel[41] | 5.43 |
| Walnut green peel[42] | 129.00 |
| *Cassia fistula* seed[43] | 182.2 |
| Lemon peel[44] | 36.74 |
| MCS (Present study) | 45.50 |
| MMCSC (Present study) | 266.67 |

were performed at different temperatures of 27, 37 and 47°C for the initial Ni(II) ions concentration of 10 mg L$^{-1}$ at constant adsorbent dose of 1 g L$^{-1}$ and an optimum pH value of 5. The percentage removal of Ni(II) ions decreases with the increase in temperature. This is mainly due to the decrease in surface activity suggesting that the adsorption between Ni(II) and MCS, MMCSC is an exothermic process.

Thermodynamic parameters such as free energy ($\Delta G^0$), enthalpy ($\Delta H^0$) and entropy ($\Delta S^0$) change of adsorption can be evaluated from the following equations

$$K_c = \frac{C_a}{C_e} \quad \ldots(12)$$

$$\Delta G^0 = - RT \ln K_c \quad \ldots(13)$$

$$\Delta G^o = \Delta H^o - T\Delta S^o \quad \ldots(14)$$

$$\ln K_c = \frac{\Delta S^0}{R} - \frac{\Delta H^0}{RT} \quad \ldots(15)$$

where, $K_c$ is the equilibrium constant (Lg$^{-1}$), $C_e$ is the equilibrium concentration (mg L$^{-1}$), $C_a$ is the amount of Ni(II) adsorbed on the adsorbent per liter of solution at equilibrium (mg L$^{-1}$), $R$ is the gas constant (8.314 kJ mol$^{-1}$ K) and T is the absolute temperature (K). The values of enthalpy change ($\Delta H^0$) and the entropy change ($\Delta S^0$) were determined from the slope and the intercept from the plot of $\ln K_c$ versus $1/T$ and are listed in Table 3.The negative value of $\Delta G^o$ implies that the adsorption of Ni(II) ions onto MCS and MMCSC was spontaneous and feasible. The $\Delta G^o$ value is more negative when decreasing the temperature, suggesting that lower temperatures favour the adsorption.The negative $\Delta H^o$ value indicates the exothermic nature of adsorption and the $\Delta S^o$ can be used to describe the randomness at the adsorbent- solution interface during the sorption.

Table 3 — Thermodynamic parameters for the adsorption of Ni(II) ions onto MCS and MMCSC

| Adsorbents | Temp (K) | Thermodynamic parameters | | |
|---|---|---|---|---|
| | | $\Delta G^0$ (kJ mol$^{-1}$) | $\Delta H^0$ (kJ mol$^{-1}$) | $\Delta S^0$ (kJ mol$^{-1}$ K$^{-1}$) |
| MCS | 300 | -4.603 | -21.88 | -0.043 |
| | 310 | -3.570 | | |
| | 320 | -3.055 | | |
| MMCSC | 300 | -7.587 | -42.09 | -0.055 |
| | 310 | -6.997 | | |
| | 320 | -5.503 | | |

**Single-stage batch adsorber**

Adsorption isotherms can be used to predict the design of single-stage batch adsorptions systems and it is already been described by Sribharathi et al.[45]. Based on the best fitting isotherm, a design of single-stage batch adsorber is shown in Fig. 7. The design purpose is to reduce the metal ion solution of volume V (L), from an initial metal ion concentration of $C_o$ to $C_e$ (mg L$^{-1}$) in the adsorption process. The amount of adsorbent used is M (g) and the solute loading on the adsorbent changes from $q_o$ =0 to $q_e$ (mg g$^{-1}$). At time t = 0, $q_0$ = 0 and as time proceeds the mass balance equated the metal ion adsorbed from the liquid to that picked up by the solid.

The mass balance equation for the sorption system in Fig. 7 can be written as

$$V(C_o - C_e) = M(q_e - q_o) = Mq_e \quad \ldots(16)$$

From adsorption studies and from model results, it was seen that the Langmuir model gave a more robust fit to equilibrium data form MCS and MMCSC. On the basis of Langmuir isotherm equation was used to predict the amount of MCS and MMCSC particles required to remove a certain percentage of Ni(II) from various volumes of solutions.

$$\text{Hence} \quad q_e = \frac{q_m K_L C_e}{1 + K_L C_e} \quad \ldots(17)$$

Since the equilibrium studies confirmed that the equilibrium data for Ni(II) ions onto MCS and MMCSC followed a Langmuir isotherm Eq. 17 substituted in Eq. 16 and it can be rearranged as:

$$\frac{M}{V} = \frac{C_o - C_e}{q_e} = \frac{C_o - C_e}{\frac{q_m K_L C_e}{1 + K_L C_e}} \quad \ldots(18)$$

Fig. 8a and b shows that the plot between the calculated amounts of MCS and MMCSC required to remove Ni(II) solution of initial concentration 50 mg L$^{-1}$ for 75%, 80%, 85%, 90% and 95% Ni(II) removal at different solution volume (1 to 10 L) for a single-stage batch adsorption system, for which the design procedure is outlined.

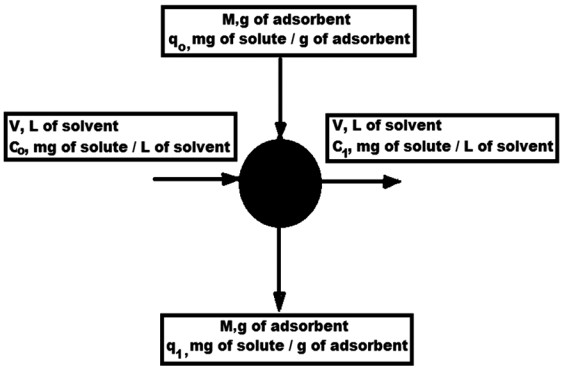


Fig. 7 — Single-stage batch adsorbent design

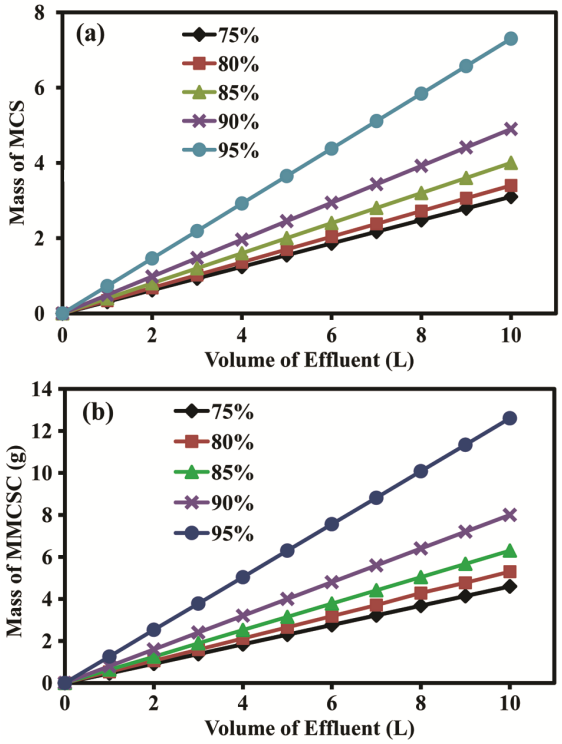


Fig. 8 — Plot between volume of Ni(II) solution treated against (a) MCS and (b) MMCSC dose for different percentage

**Removal of Ni(II) from electroplating wastewater and regeneration studies**

Batch experiments with nickel electroplating wastewater have been carried out to elucidate the applicability of both sorbents under batch mode operations. The characteristics of nickel plating wastewater are shown in Table 4. As the wastewater has a very high concentration of nickel (2400 mg L$^{-1}$), it was diluted to 10 times to conduct experiments with MCS and MMCSC. When removing Ni(II) from wastewater containing 240 mg of Ni(II) / 1000 mL,

Table 4 — Characteristics of nickel plating industry wastewater

| Parameter | Concentration |
|---|---|
| pH | 1.80 |
| Conductivity, mS $cm^{-1}$ | 15.35 |
| Total solid, mg $L^{-1}$ | 7579.00 |
| Turbidity, NTU | 30.00 |
| Chloride, mg $L^{-1}$ | 689.00 |
| Sulphate, mg $L^{-1}$ | 2036.00 |
| COD, mg $L^{-1}$ | 38.00 |
| Iron, mg $L^{-1}$ | 37.50 |
| Nickel, mg $L^{-1}$ | 2400.00 |
| Sodium, mg $L^{-1}$ | 366.00 |
| Calcium, mg $L^{-1}$ | 89.00 |
| Magnesium, mg $L^{-1}$ | 168.00 |

the optimum MCS and MMCSC doses were 10 g and 4 g reaching maximum removals of 65 (± 0.6) % and 99 (± 0.5) %, respectively. Therefore, MMCSC is more effective than MCS when treating nickel plating wastewater due to the moderate ion-exchange observed with MMCSC compared to MCS.

To determine the applicability of the adsorbent over repeated uses, 0.5 N HCl was used to regenerate the raw materials and carbon over five cycles of operation. A slight increase in the sorption of Ni(II) could be observed after each and every cycle with MMCSC, improving the recovery of Ni(II) ions. This increase in the sorption (97.0 - 99.9 %) may occur because additional surface active sites present on the sorbent surface open after repeated regeneration cycles. However, the recovery of Ni(II) decreased in MMCSC from 96.27 - 84.73 % during fifth cycle because the Ni(II) ions were strongly bound to the new opening sites. For MCS, both the adsorption and desorption values decreased rapidly. Therefore, MMCSC has a greater potential for repeated uses and the recovery of Ni(II) ions. The attrition losses were also calculated at the end of the fifth cycle. The MMCSC showed 1.0 % losses on average, while MCS showed 5 - 6 % losses at the end of the cycle during batch mode operations.

## Conclusion

The results of the present investigation show that MMCSC nanoadsorbent prepared from an agricultural waste (*Morinda citrifolia* seed) has considerable potential for the removal of Ni(II) ions from aqueous solutions. The removal of Ni(II) ions from aqueous solution strongly depends on the solution pH, contact time and carbon dose. The *Morinda citrifolia* seed podwer and its magnetic nanoparticle loaded derivative can be used to remove 45% and 99% of the Ni(II) from aqueous solutions. The presence of hydroxyl, carboxylic and Fe-O groups are confirmed by FT-IR spectroscopy. The equilibrium data fit well with Langmuir isotherm and the adsorption capacity of MMCSC is 5.8 times larger than that of MCS. Thermodynamic study shows that the adsorption was spontaneous and exothermic. A single stage batch adsorber was designed using the best fitted adsorption isotherm equation, which is Langmuir adsorption isotherm equation. The MMCSC can be regenerated and reused upto seven cycles of operation under study when compared with MCS. Therefore, it can be concluded that the MMCSC is a good and effective adsorbent for the removal of Ni(II) ions and could be used in water and wastewater treatment.

## References


1 Kumar R, Rani M, Gupta H & Gupta B, Trace metal fractionation in water and sediments of an urban river stretch, *Chem Speciat Bioavailab*, 26 (2014) 200.

2 Arain S S, Kazi T G, Arain J B, Afridi H I, Kazi A G, Nasreen S & Brahman K D, Determination of nickel in blood and serum samples of oropharyngeal cancer patients consumed smokeless tobacco products by cloud point extraction coupled with flame atomic absorption spectrometry, *Environ Sci Pollut Res*, 21 (2014) 12017.

3 Asberry H B, Kuo C Y, Gung C H, Conte E D & Suen S Y, Characterization of water bamboo husk biosorbents and their application in heavy metal ion trapping, *Micro J*, 113 (2014) 59.

4 Murugesan A, Vidhyadevi T, Kalavani S S, Baskaralingam P, Anuradha C D & Sivanesan S, Kinetic studies and isotherm modeling for the removal of $Ni^{2+}$ and $Pb^{2+}$ ions by modified activated carbon using sulfuric acid, *Environ Prog Sust Energy*, 33 (2014) 844.

5 Hannachi Y, Shapovalov N A & Hannachi A, Adsorption of Nickel from aqueous solution by the use of low-cost adsorbents, *Korean J Chem Eng*, 27 (2010) 152.

6 Hannachi Y, Shapovalov N A & Hannachi A, Adsorption of nickel from aqueous solution by the use of low-cost adsorbents, *Kore J Chem Eng*, 27 (2010) 152

7 Jiang R, Tian J, Zheng H, Qi J, Sun S & Li X, A novel magnetic adsorbent based on waste litchi peels for removing Pb(II) from aqueous solution, *J Environ Manage*, 155 (2015) 24.

8 Dabrowski A, Hubicki Z, Podkoscielny P & Robens E, Selective removal of the heavy metal ions from waters and industrial wastewaters by ion-exchange method, *Chemosphere*, 56 (2004) 91.

9 Fu F & Wang Q, Removal of heavy metal ions from wastewaters: A review, *J Environ Manage*, 92 (2011) 407.

10 Mishra S & Verma N, Surface ion imprinting-mediated carbon nanofiber-grafted highly porous polymeric beads: Synthesis and application towards selective removal of aqueous Pb(II), *Chem Eng J*, 313 (2017) 1142.

11 Kanwal S, Naeem H K, Batool F, Mirza A, Abdelrahman E A, Sharif G, Maqsood F, Mustaqeem M & Ditta A, Adsorption potential of orange rind-based nanosorbents for the removal of cadmium(II) and chromium(VI) from

contaminated water, *Environ Sci Pollut Res*, 30 (2023) 110658.
12 Peighambardoust S J, Foroutan R, Peighambardoust S H, Khatooni H & Ramavandi B, Decoration of Citrus limon wood carbon with $Fe_3O_4$ to enhanced $Cd^{2+}$ removal: A reclaimable and magnetic nanocomposite, *Chemosphere*, 282 (2021) 131088.
13 Zhang Z, Wang T, Zhang H, Liu Y & Xing B, Adsorption of Pb(II) and Cd(II) by magnetic activated carbon and its mechanism, *Sci Total Environ*, 757 (2021) 143910.
14 Prabu D, Kumar P S, Varsha M, Sathish S, Vijai Anand K & Mercy J, Potential of nanoscale size zero valent iron nanoparticles impregnated activated carbon prepared from palm kernel shell for cadmium removal to avoid water pollution, *Int J Environ Anal Chem*, 102 (2022) 7224.
15 Khalil A, Salem M, Ragab S, Sillanpaa M & El Nemr A, Orange peels magnetic activate carbon (MG-OPAC) composite formation for toxic chromium absorption from wastewater, *Sci Rep*, 13 (2023) 3402.
16 Bagherzadeh M, Aslibeiki B & Arsalani N, Preparation of $Fe_3O_4$/vine shoots derived activated carbon nanocomposite for improved removal of Cr(VI) from aqueous solutions, *Sci Rep*, 13 (2023) 3960.
17 Jaber L, Ihsanullah I, Almanassra I W, Backer S N, Abushawish A, Khalil A K A, Alawadhi H, Shanableh A & Atieh M A, Adsorptive removal of lead and chromate ions from water by using iron-doped granular activated carbon obtained from coconut shells, *Sustainability*, 14 (2022) 10877.
18 Kamal K H, Attia M S, Ammar N S & Abou-Taleb E M, Kinetics and isotherms of lead ions removal from wastewater using modified corncob nanocomposite, *Inorg Chem Commun*, 130 (2021) 108742.
19 Sharma R, Sarswat A, Pittman C U & Mohan D, Cadmium and lead remediation using magnetic and non-magnetic sustainable biosorbents derived from Bauhinia purpurea pods, *RSC Adv*, 7 (2017) 8606.
20 Asadollahzadeh H, Ghazizadeh M & Manzari M, Developing a magnetic nanocomposite adsorbent based on carbon quantum dots prepared from Pomegranate peel for the removal of Pb(II) and Cd(II) ions from aqueous solution, *Anal Methods Environ Chem J*, 4 (2021) 33.
21 Freundlich H M F, Over the adsorption in solution, *J Phys Chem*, 57 (1906) 385.
22 Langmuir I, The adsorption of gases on plane surfaces of glass, mica and platinum, *J Am Chem Soc*, 40 (1918) 1361.
23 Weber T W & Chakraborty R K, Pore and solid diffusion models for fixed-bed adsorbers, *J Am Inst Chem Eng*, 20 (1974) 228.
24 Temkin M J & Pyzhev V, Recent modifications to Langmuir isotherms, *Acta Physicochim URSS*, 12 (1940) 217.
25 Redlich O & Peterson D L, A useful adsorption isotherm, *J Phys Chem*, 63 (1959) 1024.
26 Sips R, On the structure of a catalyst surface, *J Chem Phys*, 16 (1948) 490.
27 Dubinin M M & Radushkevich L V, Equation of the characteristic curve of activated charcoal, *Chem Zentr*, 1 (1947) 875.
28 Kundu S & Gupta A K, Arsenic adsorption onto iron oxide-coated cement (IOCC): Regression analysis of equilibrium data with several isotherm models and their optimization, *Chem Eng J*, 122 (2006) 93.
29 Helfferich F, *Ion exchange*, McGraw-Hill Book Co. New York (1962).
30 Chen H, Dai G, Zhao J, Zhong A, Wu J & Yan H, Removal of copper(II) ions by a biosorbent--Cinnamomum camphora leaves powder, *J Hazard Mater*, 177 (2010) 228.
31 Panneerselvam P, Morad N & Tan K A, Magnetic nanoparticle ($Fe_3O_4$) impregnated onto tea waste for theremoval of nickel(II) from aqueous solution, *J Hazard Mater*, 186 (2011) 160.
32 Sudha R, Latha K & Jayalakshmi R, Isotherm studies on removal of lead(II) ions from wastewater by magnetic carbon synthesised from Euphorbia hirta leaf extract, *Indian J Chem Technol*, 30 (2023) 672.
33 Lee C H & Lee C H, A study on nickel hydroxide crystallization characteristics, *Korean J Chem Eng*, 22 (2005) 712.
34 Sudha R, Srinivasan K & Premkumar P, Removal of nickel(II) from aqueous solution using Citrus Limettioides peel and seed carbon, *Ecotox Environ Saf*, 117 (2015) 115.
35 Rao R A K & Ikram S, Sorption studies of Cu(II) on gooseberry fruit (Emblica officinalis) and its removal from electroplating wastewater, *J Desal*, 277 (2011) 390.
36 Anitha D, Ramadevi A & Seetharaman R, Biosorptive removal of nickel(II) from aqueous solution by mangosteen shell activated carbon, *Mater Today: Proc*, 45 (2021) 718.
37 Paula R B D, Dias P I, Silva P M, Adeodato V M G & Freire B R, Activated carbons from passion fruit shells in adsorption of multimetal wastewater, *Environ Sci Pollut Res*, 29 (2022) 1446.
38 Karapinar H S, Adsorption performance of activated carbon synthesis by $ZnCl_2$, KOH, $H_3PO_4$ with different activation temperatures from mixed fruit seeds, *Environ Technol*, 43 (2022) 1417.
39 Mittal J, Ahmad R, Mariyam A, Gupta V K & Mittal A, Expeditious and enhanced sequestration of heavy metal ions from aqueous environment by papaya peel carbon: A green and low-cost adsorbent, *Desal Water*, 210 (2021) 365.
40 Sadat S M O, Kucukcongar S & Turkyilmaz M, Nickel adsorption from waters onto $Fe_3O_4$/sugar beet pulp nanocomposite, *Int J Phytoremed*, 25 (2023) 572.
41 Manjuladevi M, Anitha R & Manonmani S, Kinetic study on adsorption of Cr(VI), Ni(II), Cd(II) and Pb(II) ions from aqueous solutions using activated carbon prepared from Cucumis melo peel, *Appl Water Sci*, 8 (2018) 36.
42 Yu M, Zhu B, Yu J, Wang X, Zhang C & Qin Y, A biomass carbon prepared from agricultural discarded walnut green peel: Investigations into its adsorption characteristics of heavy metal ions in wastewater treatment, *Biomass Convers Bioref*, 13 (2022) 12833.
43 Hemavathy R R V, Kumar P S, Suganya S, Swetha V & Varjani S J, Modelling on the removal of toxic metal ions from aquatic system by different surface modified Cassia fistula seeds, *Bioresour Technol*, 281 (2019) 1.
44 Villen-Guzman M, Gutierrez-Pinilla D, Gomez-Lahoz C, Vereda-Alonso C, Rodriguez-Maroto J M & Arhoun B, Optimization of Ni(II) biosorption from aqueous solution on modified lemon peel, *Environ Res*, 179 (2019) 108849.
45 Sribharathi S, Kavitha G & Sudha R, Synthesis of magnetic activated carbon from Citrus hystrix (Kaffir lime or Kolumichai) leaves with excellent Pb(II) adsorption performance towards electroplating wastewater, *Indian J Chem Technol*, 29 (2022) 229.